

# Application of Vibration Signals in Medical Drill Wear Monitoring

Zrinka Murat, Danko Brezak, Dubravko Majetic and Toma Udiljak

**Abstract**— Usage of worn drills in medical interventions has highly negative influence on the heat generation which can consequently result in thermal necrosis of bone tissue and prolonged postoperative healing process. Precise real time direct measurement of cutting tool wear level during machining process is not possible. Therefore, the main goal of this study was to identify wear level using indirect monitoring technique based on tool wear features extracted from vibration signals measured during drilling process. Experiment was based on fresh bovine bone samples which were drilled with standard surgical drill used for bone and joint surgery applications. Three drill wear levels in combination with the 12 different machining parameter sets were analyzed. Drill wear features were analyzed using Radial Basis Function Neural Network algorithm with Gaussian activation function. The best overall classification precision regarding all three wear levels was around 79%, while the third and the highest wear level analyzed in this study was exactly classified in 95% of all test samples.

**Index Terms**—drilling, thermal osteonecrosis, vibrations, wear modeling

## I. INTRODUCTION

BONE is a complex biological tissue with organic and mineral elements whose interactions result in unique mechanical and thermal properties. Unlike its mechanical characteristics, biochemical processes which occur in bone tissue during heat exposure and its thermodynamic characteristics are still not clearly described. However, negative thermal impact on bone tissue caused by drilling process is known for a long time. A number of studies performed to determine maximum allowable drilling temperature and exposure period beyond which thermal osteonecrosis occurs have been published. Results have confirmed inversely proportional relationship between those two parameters. Erikson and Albrektsson [1] have noticed bone thermal damages at 47°C after 1 min of exposure in their in vivo experiments on rabbits. Hillery and Shuaib [11] concluded that significant damages occurred at 55°C after

the exposure period longer than 30s. Karmani [3] points out that there is no common conclusion about minimum drilling temperature which causes thermal osteonecrosis or ideal conditions for defining that temperature. He agrees with the results and conclusions presented in [4], which coincide with his average critical temperature value of 50°C and the exposure time of 30s.

There are several factors influencing heat generation in bone drilling – drill design, machining parameters, drilling depth (cortical thickness), cooling technique and drill wear rate [5]. Drill wear rate has strong influence on heat generation during bone drilling. Mathews and Hirsch [6] have confirmed this claim several decades ago when they compared new drills with those used to drill more than 200 holes. As expected, worn drills accomplished higher temperatures during drilling. Importance of a drill wear rate on bone thermal damages has been emphasized in [7] where three types of drills were compared: new one, drill which drilled 600 holes, and drill which were used for several months. The results have shown important differences in mean temperature rise values and authors suggested drill replacement after every surgical intervention. The same negative influence of drill wear have been reported in [8 - 10] where the temperature rise and thermal osteonecrosis is noticed after 25, 30 and 40 drilled holes, respectively.

Although there have been many papers published in the past several decades considering tool wear monitoring in industrial applications [11], quality analyses in the field of medical drilling are still missing. Industrial drilling dynamics usually differ from the one related to the medical applications in view of different drill characteristics, machining parameters, and workpiece material characteristics. So it should be interesting to see is it possible to just copy some of the proposed industrial solutions and implement them in medical drill wear monitoring. First analyses [12, 13] imply the applicability of multi-sensor concept and advanced decision algorithms in on-line medical drill wear monitoring. They have also confirmed the necessity of further research engagements in this field.

The analysis performed in this research is a logical continuation of the activities and results presented in two previously cited papers. In this study, the potential of drill wear features extracted from vibration signals to precisely classify three drill wear levels (sharp, medium worn and worn drill) has been analyzed. Classification potential of chosen drill wear futures were analyzed using Radial Basis Function (RBF) neural network.

Manuscript received December 8, 2017; revised January 3, 2018. This work was supported by the Croatian Science Foundation under the project number IP-09-2014-9870.

Z. Murat is with the Faculty of Mechanical Engineering and Naval Architecture, University of Zagreb, Croatia (e-mail: zrinka.murat@fsb.hr).

D. Brezak is with the Faculty of Mechanical Engineering and Naval Architecture, University of Zagreb, Croatia (phone: +385 1 6168357, fax: +385 1 6168351; e-mail: danko.brezak@fsb.hr).

D. Majetic is with the Faculty of Mechanical Engineering and Naval Architecture, University of Zagreb (e-mail: dmajetic@fsb.hr).

T. Udiljak is with the Faculty of Mechanical Engineering and Naval Architecture, University of Zagreb (e-mail: toma.udiljak@fsb.hr).

## II. EXPERIMENTAL SETUP, SIGNAL PROCESSING AND FEATURES EXTRACTION

### A. Experimental Setup

Bone drilling experiment was performed with the 3-axis bench-top mini milling machine adjusted for the purpose of this research (Fig. 1). The machine has been retrofitted with the 0.4 kW (1.27 Nm) permanent magnet synchronous motors with integrated incremental encoders (type Mecapion SB04A), corresponding motor controllers (DPCANIE-030A400 and DPCANIE-060A400), ball screw assemblies, and LinuxCNC open architecture control (OAC) system.

Triaxial accelerometer type Kistler 8688A50 with the corresponding coupler type 5134B was installed near the front bearing of the motor spindle in order to avoid any unnecessary vibration signal attenuation. Vibrations were measured in the range of 0.5 - 5000 Hz in three mutually perpendicular axes, where one axis was collinear with the drill longitudinal axis.

The experiment is characterized with the remaining following features:

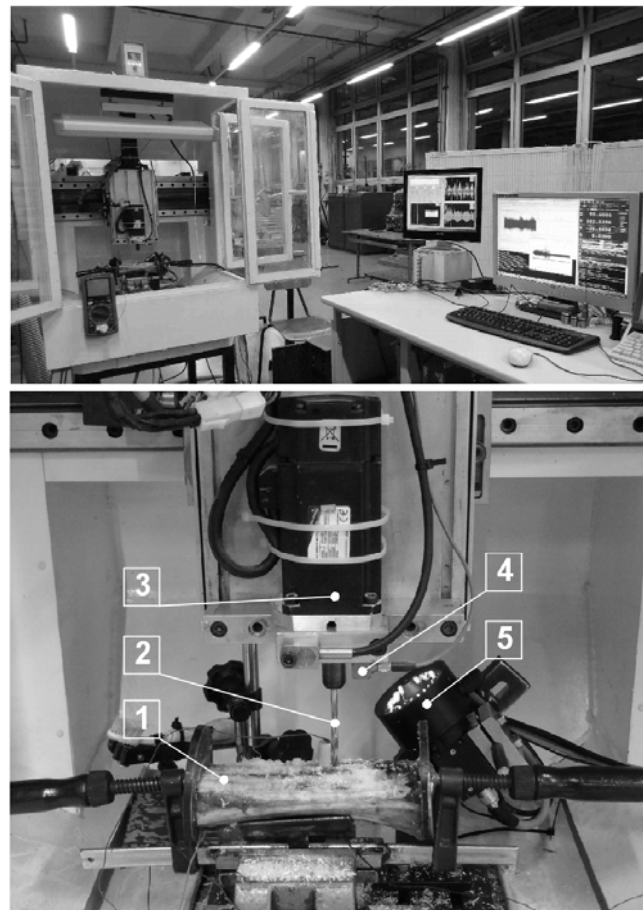
- *Komet Medical* surgical drill type S2727.098 (4.5 mm in a diameter);
- three different cutting edges wear conditions (Fig. 2) – sharp drill (SD), medium worn drill (MD) and worn drill (WD);
- 12 combinations of cutting speeds (10; 30; 50 m/min), and feed rates (0.01; 0.03; 0.05; 0.1 mm/rev) – cutting speeds correspond to spindle speeds of 707.4 rpm, 2122.1 rpm and 3536.8 rpm, respectively;
- each combination of machining parameters were randomly repeated 10 times;
- fresh bovine tibia with average diaphysis cortical thickness (drilling depth) of 7.8 mm.

### B. Signal Processing and Drill Wear Features Extraction

All signals were measured with 100 kHz sampling rate within a period of 2 seconds. Raw measured signals have been analyzed in the frequency domain using the Fast Fourier Transform (FFT) algorithm. After transforming signal from time to frequency domain frequency bandwidth, defined by the sensor measuring range (0.5 – 5000 Hz), was divided into 23 frequency ranges of different widths (5, 10, 20, ..., 90, 100, 200, ..., 900, 1000, 1500, 2500, 5000) Hz; and the energy of every range was used as a drill wear feature in the first phase of the classification process. Energy is calculated from the expression

$$\psi^2 = \int_{f_L}^{f_U} S_y df \quad (1)$$

where  $S_y$  is one-sided PSD function of the AE signal, while  $f_L$  and  $f_U$  are lower and upper frequency values chosen to reflect the energy in the range of interest [15]. Altogether 9 groups of features were used in this analysis (Table I). Four of them were extracted directly from three types of vibration signals - energies related to different frequency ranges of every vibration signal individually (X, Y and Z) and sum of energies of all three signals ( $XYZ_{SUM}$ ). The remaining five



1) Bone specimen  
2) Surgical drill  
3) Main spindle motor  
4) Vibration sensor (accelerometer)  
5) Industrial CCD camera with telecentric lens

Fig. 1. Experimental setup

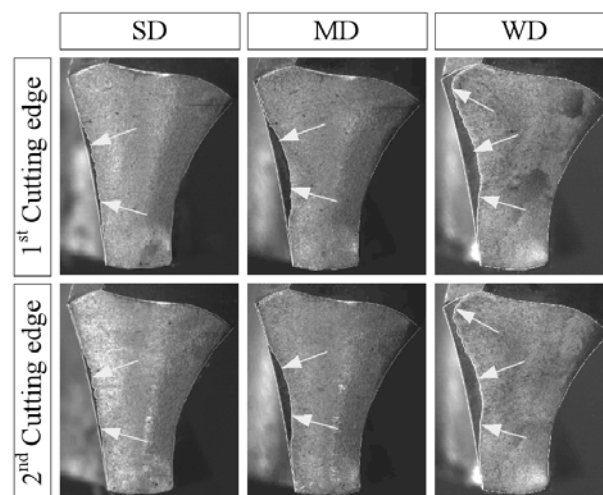


Fig. 2. Images of both cutting edges after drilling with observable (arrows pointing to) flank wear zone - sharp drill (SD), medium worn drill (MD) and worn drill (WD). Flank wear areas of those three drill wear levels were: (0 – 0.105) mm<sup>2</sup> for SD drill, (0.208 – 0.232) mm<sup>2</sup> for MD drill and (0.386 – 0.473) mm<sup>2</sup> for WD drill.

groups were obtained from mutual combinations of the first four. Together with the two machining parameters (drill cutting speed and feed rate), those features (energies) were used as RBF NN inputs.

TABLE I  
LIST OF DRILL WEAR FEATURES

Feature group label	Description
X	Energies of the frequency spectrum of the vibration signal in the X-axis direction related to different frequency ranges
Y	Energies of the frequency spectrum of the vibration signal in the Y-axis direction related to different frequency ranges
Z	Energies of the frequency spectrum of the vibration signal in the Z-axis direction related to different frequency ranges
XYZ <sub>SUM</sub>	Sum of the energies of the frequency spectrum of vibration signals in the X, Y, Z-axis direction related to different frequency ranges
XY	Combination of X and Y
XZ	Combination of X and Z
YZ	Combination of Y and Z
XYZ	Combination of X, Y and Z
XYZ-XYZ <sub>SUM</sub>	Combination of X, Y, Z and XYZ <sub>SUM</sub>

Every feature combination from the table also imply the usage of drill cutting speed and feed rate as two additional input parameters of the RBF NN classifier.

### III. RBF NEURAL NETWORK ALGORITHM

Utilized NN algorithm is based upon a well-known feedforward three-layered RBF NN architecture, where the matrix/vector of synaptic weights  $\mathbf{c}$  is calculated in the learning phase using the expression

$$\mathbf{c} = \mathbf{H}^+ \mathbf{y}, \quad (2)$$

where  $\mathbf{y}$  stands for the matrix/vector of desired output values and  $\mathbf{H}^+$  is Moore – Penrose pseudoinverse of the matrix of hidden layer neuron RBF outputs or activation function outputs ( $\mathbf{H}$ ). The pseudoinverse is defined as follows

$$\mathbf{H}^+ = (\mathbf{H}^T \mathbf{H})^{-1} \mathbf{H}^T. \quad (3)$$

In the testing phase, the matrix of desired output values  $\mathbf{y}$  is obtained from the expression

$$\mathbf{y} = \mathbf{H} \mathbf{c}. \quad (4)$$

Elements of matrix  $\mathbf{H}$  are determined according to the expression [14]

$$H_{ij} = e^{-\frac{1}{2}r_{ij}^2}, \quad i = 1, \dots, N, \quad j = 1, \dots, K, \quad (5)$$

where  $r_{ij}$  is the Mahalanobis distance between vector composed from  $i$ th element of all input vectors (tool wear features) and  $j$ th hidden layer neuron. Squared Mahalanobis distance is calculated using the expression

$$r_{ij}^2 = (\mathbf{x}_i - \mathbf{t}_j)^T \boldsymbol{\Sigma}_j^{-1} (\mathbf{x}_i - \mathbf{t}_j), \quad (6)$$

where  $\boldsymbol{\Sigma}_j$  is a covariance matrix belonging to the group of learning samples that are connected to the  $j$ th hidden layer

neuron,  $\mathbf{x}_i$  is the  $L$ -dimensional vector composed from  $i$ th element of all  $L$  input vectors and  $\mathbf{t}_j$  is  $L$ -dimensional vector of the  $j$ th hidden layer neuron center. Covariance matrix is quadratic matrix with non-zero elements (squared  $\boldsymbol{\sigma}$  vector components) on main diagonal and zeros elsewhere,

$$\boldsymbol{\Sigma}_j = \begin{bmatrix} \sigma_{1j}^2 & 0 & 0 \\ 0 & \ddots & 0 \\ 0 & 0 & \sigma_{Lj}^2 \end{bmatrix}. \quad (7)$$

Vector  $\boldsymbol{\sigma}$  is defined according to the expression

$$\sigma_{gj} = 0.5 \cdot \min |t_{gj} - t_{gp}|, \quad p = j, 1, \dots, K, \quad p \neq j, \quad (8)$$

where  $t_{gj}$  is the  $g$ th component of the  $j$ th hidden layer neuron center vector, and  $t_{gp}$  is the  $g$ th component of  $p$  remaining hidden layer neuron center vector.

The number hidden layer neurons ( $K$ ) can be lower or equal to the number of learning samples ( $N$ ). In this study, hidden layer is structured in a way that for every learning sample a hidden layer neuron was formed ( $K=N$ ). This means that each hidden layer neuron center was defined by one learning sample ( $\mathbf{t}_j = \mathbf{x}_i, i = j = 1, \dots, N$ ).

### IV. DATA SETS PREPARATION AND CLASSIFICATION PROCEDURE

Since 12 combinations of machining parameters were combined with three drill wear levels, and measurements for these 36 combinations were randomly repeated 10 times, altogether 360 data sets have been recorded. Half of those data sets were used in the learning phase, and the remaining sets were divided in five equal subsets (five tests) used in the testing phase of the RBF NN classifier. In other words, five out of 10 samples of repetitive measurements for each combination of machining parameters were used in the learning phase, and the remaining five participated in the formation of five tests.

In order to find the best feature combination drill wear classification process was performed in three steps (Fig. 3.). In the first step, energies from all 23 chosen frequency ranges were analyzed by the RBF NN for each feature group individually. The results were compared using Classification Success Rate (CSR) factor defined as a ratio of correctly

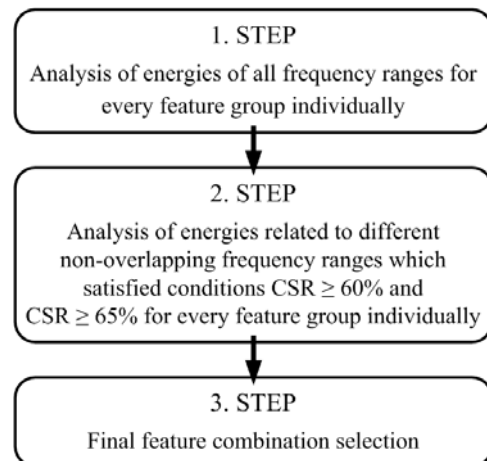


Fig. 3. The best feature combination selection process

classified samples over all test samples. Only those energies from frequency ranges which satisfied predefined  $CSR \geq 60\%$  and  $CSR \geq 65\%$  criteria participated in the second step of the classification process. Those CSR values were determined based on the fact that none of the features satisfied  $CSR \geq 70\%$ .

In the second step, classification potential of every feature group was additionally analyzed by combining chosen energies from different non-overlapping ranges. Non-overlapping ranges were chosen based on achieved CSR results, i.e., range with higher CSR had higher selection priority. This means that feature from the range which satisfied CSR condition was omitted from further classification process if it was completely or partially overlapped with another range of higher priority.

At the end, in the third step the best results of all feature groups compared mutually and the best feature group or combination was selected.

### V. RESULTS AND DISCUSSION

Results for both CSR values ( $CSR \geq 60\%$ ,  $CSR \geq 65\%$ ) are presented in Table II and III, respectively. Two groups of features accomplished very similar results. Both groups imply the usage of all three types of vibration signals and their combination. Classification potential of the feature combination which achieved the best result (XYZ-XYZ<sub>SUM</sub> for  $CSR \geq 65\%$  condition) was additionally analyzed for every drill wear level and the results are presented in Table IV. They reveal an interesting fact that the RBF NN classifier did not manage to satisfactory identify second or "medium worn drill" wear level. Some 60% of misclassified

samples were classified in WD level and the rest in SD level. The CSR value of 55% indicates practical inapplicability of the analyzed approach in MD wear level identification. However, this experiment should be repeated with different surgical drills and bone samples of similar cortical bone hardness before drawing any final conclusions. This will be done in the next study.

Despite very low performance in MD wear level classification, features extracted from vibration signals still managed to correctly identify the highest or WD drill wear level in 95% of samples. This indicates potential applicability of vibration signals in medical drill wear monitoring, especially if used in combination with other types of indirect monitoring signals.

### REFERENCES

- [1] A.R. Eriksson and T. Albrektsson, "Temperature Threshold Levels for Heat-Induced Bone Tissue Injury: A Vital-Microscopic Study in the Rabbit," *Journal of Prosthetic Dentistry*, vol. 50, no. 1, pp. 101-107, Jul. 1983.
- [2] M.T. Hillery and I. Shuaib, "Temperature effects in the drilling of human and bovine bone," *Journal of Materials Processing Technology*, vol. 92-93, pp. 302-308, Aug. 1999.
- [3] S. Karmani, "The thermal properties of bone and the effects of surgical intervention," *Current Orthopaedics*, vol. 20, no. 1, pp. 52-58, Feb. 2006.
- [4] J. Lundskog, "Heat and bone tissue. An experimental investigation of the thermal properties of bone and threshold levels from thermal injury," *Scandinavian Journal of Plastic and Reconstructive Surgery*, vol. 9, pp. 1-80, Jan 1972.
- [5] G. Augustin, T. Zigman, S. Davila, T. Udiljak, T. Staroveski, D. Brezak, and S. Babic, "Cortical bone drilling and thermal osteonecrosis," *Clinical Biomechanics*, vol. 27, no. 4, pp. 313-325, May 2012.
- [6] L. S. Mathews and C. Hirsch, "Temperature measured in human cortical bone when drilling," *The Journal of Bone Joint Surgery*, vol. 54, no. 2, pp. 297-308, Apr. 1972.
- [7] W. Allan, E.D. Williams and C.J. Kerawala, "Effects of repeated drill use on temperature of bone during preparation for osteosynthesis self-tapping screws," *British Journal of Oral and Maxillofacial Surgery*, vol. 43, no. 4, pp. 314-319, Aug. 2005.
- [8] G.E. Chacon, D.L. Bower, P.E. Larsen, E.A. McGlumphy, and F.M. Beck, "Heat Production by 3 Implant Drill Systems After Repeated Drilling and Sterilization", *Journal of Oral and Maxillofacial Surgery*, vol. 64, no. 2, pp. 265-269, Feb. 2006.
- [9] T. P. Queiroz, F. Á. Souza, R. Okamoto, R. Margonar, V. A. Pereira-Filho, I. R. Garcia, and E. H. Vieira, "Evaluation of Immediate Bone-Cell Viability and of Drill Wear After Implant Osteotomies: Immunohistochemistry and Scanning Electron Microscopy Analysis," *Journal of Oral and Maxillofacial Surgery*, vol. 66, no. 6, pp. 1233-1240, Jun. 2008.
- [10] R. M. Jochum and P. A. Reichart, "Influence of multiple use of Timedur® – titanium cannon drills: thermal response and scanning electron microscopic findings," *Clinical Oral Implants Research*, vol. 11, no. 2, pp. 139-143, Apr. 2000.
- [11] E. Jantunen, "A summary of methods applied to tool condition monitoring in drilling," *International Journal of Machine Tools & Manufacture*, vol. 42, no. 9, pp. 997-1010, Jul. 2002.
- [12] T. Staroveski, D. Brezak, V. Grdan, and T. Bacek, "Medical Drill Wear Classification Using Servomotor Drive Signals and Neural Networks," *Lecture Notes in Engineering and Computer Science*, vol. 1, pp. 599-603, 2014.
- [13] T. Staroveski, D. Brezak and T. Udiljak, "Drill Wear Monitoring in Cortical Bone Drilling," *Medical Engineering & Physics*, vol. 37, no. 6, pp. 560-566, Jun. 2015.
- [14] B. Novakovic, D. Majetic, and M. Siroki, *Artificial Neural Networks*. Zagreb: University of Zagreb, Faculty of Mechanical Engineering and Naval Architecture, 1998.
- [15] C. Scheffer, H. Kratz, P.S. Heyns and F. Klocke, "Development of a tool wear-monitoring system for hard turning," *International Journal of Machine Tools & Manufacture*, vol. 43, no. 10, pp. 973-985, Aug. 2003.

TABLE II  
 CLASSIFICATION RESULTS ACHIEVED WITH FEATURES WHICH INDIVIDUALLY SATISFIED CONDITION  $CSR \geq 60\%$  (ACCURATELY CLASSIFIED SAMPLES IN %)

Feature	TEST					Avg. (CSR)
	T1	T2	T3	T4	T5	
Y	75.0	63.9	55.6	50.0	55.6	60.0
XY	75.0	83.3	69.4	58.3	63.9	70.0
YZ	72.2	63.9	61.1	63.9	63.9	65.0
XZ	66.7	75.0	77.8	69.4	69.4	71.7
XYZ	66.7	80.6	77.8	72.2	83.3	76.1
XYZ-XYZ <sub>SUM</sub>	77.8	66.7	66.7	75.0	69.4	71.1

TABLE III  
 CLASSIFICATION RESULTS ACHIEVED WITH FEATURES WHICH INDIVIDUALLY SATISFIED CONDITION  $CSR \geq 65\%$  (ACCURATELY CLASSIFIED SAMPLES IN %)

Feature	TEST					Avg. (CSR)
	T1	T2	T3	T4	T5	
YZ	72.2	66.7	66.7	52.8	72.2	66.1
XYZ	66.7	69.4	66.7	77.8	72.2	70.6
XYZ-XYZ <sub>SUM</sub>	77.8	80.6	80.6	77.8	77.8	78.9

TABLE IV  
 CLASSIFICATION RESULTS ACHIEVED WITH THE BEST FEATURE (XYZ-XYZ<sub>SUM</sub>) WHICH SATISFIED CONDITION  $CSR \geq 65\%$  (ACCURATELY CLASSIFIED SAMPLES IN %)

Drill Wear Level	TEST					Avg. (CSR)
	T1	T2	T3	T4	T5	
SD	100.0	75.0	83.3	83.3	91.7	86.7
MD	41.7	66.7	66.7	50.0	50.0	55.0
WD	91.7	100.0	91.7	100.0	91.7	95.0